ASTRONOMY & ASTROPHYSICS
SUPPLEMENT SERIES

APRIL I **1997**, PAGE 167

Astron. Astrophys. Suppl. Ser. **122,** 167-176 (1997)

Atomic data from the IRON Project

XX. Photoionization cross sections and oscillator strengths for Fe I

M.A. Bautista

Department of Astronomy, The Ohio State University, 174 West 18th Avenue, Columbus, OH 43210-1106, U.S.A.
internet: bautista@payne.mps.ohio-state.edu

Received May 21; accepted July 19, 1996

Abstract. Large-scale close coupling calculations for photoionization cross sections and dipole transition probabilities for Fe I are reported. The calculation included 52 LS terms of the target ion Fe II dominated by the configurations $3d^6 4s$, $3d^7$, $3d^6 4p$, $3d^5 4s^2$, and $3d^5 4s4p$. The eigenfunction expansion of Fe II accounts for the photoionization of the outer 4s subshell, as well as the open inner 3d subshell, of the ground state $3d^6 4s^2\ {}^5D$ of Fe I. The results include energy levels for 1,117 LS bound states of Fe I, with $n \leq 10$ and $\ell \leq 7$, 32 316 dipole oscillator strengths for transitions among the LS multiplets, and detailed photoionization cross sections, with extensive resonance structures, for all computed bound states. The present photoionization cross section for the ground state is up to three orders of magnitude higher than earlier results from central field type approximations, but it agrees reasonably well with the cross section previously calculated using many-body perturbation theory.

Key words: atomic data — ultraviolet: general — infrared: general

1. Introduction

Low ionization stages of iron, owing to their rich and complex structure and their relatively high abundance, dominate certain wavelength regions in the spectra of a variety of stellar and non-stellar objects, as well as the interstellar medium. For example, Fe I contributes significantly to the UV opacity in the solar atmosphere (e.g. Bell et al. 1994) and it is possible that the presence of autoionizing resonances of this ion might be a major contributor to observed features in the absorption spectra. The interpretation and modeling of these observations rely almost entirely on theoretical calculations which, until the recent advances made under the Opacity Project (OP, Seaton et al. 1994) and the IRON Project (IP, Hummer et al. 1993), could not be obtained either with sufficient accuracy or on the large scale needed for a full determination of the relevant astrophysical parameters. However, some of the OP calculations, particularly for the low ionization stages of IRON, including Fe I, are of insufficient accuracy. For example, earlier R-matrix calculations for Fe I were carried out by Sawey & Berrington (1992), but they included only terms dominated by the ground configuration of Fe II and therefore do not accurately represent the coupling effects (for example, their calculations did not obtain the ground state of Fe I). Other calculations of photoionization cross sections for Fe I have been carried out in central field type approximations (Reilman & Manson 1979; Verner et al. 1993), and using the many-body perturbation method by Kelly & Ron (1972) and Kelly (1972), but are limited to just the ground state. Moreover, these central field calculations ignore the coupling effects and resonances which led to an underestimation of the photoionization cross section by more than *three orders of magnitude* as shown in a previous paper (Bautista & Pradhan 1995). The many-body perturbation calculation by Kelly considers a limited number of coupling effects including those that result from the $3d^6 4s^2$ configuration and reproduces some of the overall structure of the photoionization cross section, but neglects correlations from the $3d^6 4s4p$ configuration that are of considerable importance (see Sect. 4.3). Kelly's computations also did not allow for most of the narrow autoionization resonances that converge onto each of the ionization thresholds and make an important contribution to the cross section in the low energy region. In the absence of reliable and extensive radiative data for Fe I, theoretical calculations and modeling work that involve this ion, like computations of stellar opacities and modeling of the ionization equilibrium of iron, have been severely limited and some authors even prefer to exclude this ion from their models (e.g. LeBlanc & Michaud 1995).

It is one of the aims of the IP to carry out improved calculations for the low ionization stages of iron

(Bautista et al. 1995; Pradhan 1995) and results for some of them have already been reported, e.g. Fe II (Nahar & Pradhan 1994; Nahar 1995a), Fe III (Nahar 1995b), and Fe V (Bautista 1996), and are expected to become available soon from TOPbase at CDS (Cunto et al. 1993; Mendoza 1995, private communication).

2. Target expansion

In the close coupling (CC) approximation the total wave function of the (e + ion) system is represented as

$$\Psi(E; SL\pi) = \mathcal{A} \sum_i \chi_i \theta_i + \sum_j c_j \Phi_j, \quad (1)$$

where $\mathcal{A}$ is the antisymmetrization operator, χ_i is the target ion wave function in a specific state $(LS\pi)_i$, θ_i is the wave function for the free electron, and Φ_j are short range correlation functions for the bound (e + ion) system. Accurate computations for Fe I must allow for channel couplings among many states of the target ion Fe II for at least three reasons. First, the configuration interaction (CI) between the numerous low lying LS terms is important. Second, it is known that strong dipole couplings between opposite parity terms within the target ion give rise to large photoexcitation-of-core (PEC) resonances at corresponding incident photon frequencies (Yu & Seaton 1987). Third, the photoionization channels

corresponding to the ionization of the open inner 3d shell are likely to contribute considerably to the total cross section. This requires that terms dominated by the configurations $3d^5 4s^2$ and $3d^5 4s4p$ of Fe II should also be included. The photoionization of Fe I is considered as

$$h\nu + \mathrm{FeI} \rightarrow \quad (2)$$

$$\mathrm{e} + \mathrm{FeII}\ (3d^6 4s + 3d^7 + 3d^6 4p + 3d^5 4s^2 + 3d^5 4s4p).$$

A total of 52 LS terms of the target ion Fe II were included in the close-coupling (CC) expansion for this calculation. Table 1 lists all the coupled LS terms in the present calculations, as well as the correlation configurations included for CI. The atomic structure program SUPERSTRUCTURE (Eissner et al. 1974; Nussbaumer & Storey 1978) was used to optimize the target wavefunctions. Table 2 compares the calculated energies for the 52 terms of Fe II included in the calculation. In general, the target energies obtained were within 10% of the experimentally observed energies for the 52 terms, with few exceptions. A further indication of the accuracy of the target wavefunctions was the good agreement (< 10%) between the length and the velocity dipole oscillator strengths between opposite parity terms of Fe II.

3. Radiative calculations

The second summation in the CC expansion (Eq. 1) represents short range correlation functions that need to be optimized in order to obtain accurate (e + ion) wavefunctions and to avoid pseudo-resonances that result when the two summations are not consistent (Berrington et al. 1987). In the present work, the set of Φ_j functions was optimized for each set of symmetries of Fe I with spin multiplicity $(2S + 1) = 1$, 3, 5, and 7, in a careful manner so as to obtain accurate energies of the bound states of Fe I, as compared to experimental energies. In order to keep the calculations computationally tractable one tries to limit the bound channel set to be as small as possible. However, for Fe I the sets of $(N + 1)$-electron functions needed were very large for symmetries with multiplicity 1 and 3, and had to be truncated in view of our present computational capabilities on the Cray Y-MP with 64 MW memory and 2 Gb disk space limit for the diagonalization of the dipole matrix in the STGH program. This computational constraint affected the accuracy of the results for the singlet and the triplet symmetries, as discussed in the next section. The present calculation for quintets and septets symmetries included a total of 56 $(N+1)$-electron functions which produced nearly 1650 configurations, 150 channels, and a Hamiltonian matrix with a maximum dimension of nearly 2000. For singlets and triplets symmetries 65 $(N + 1)$-electron functions were included which gave rise to almost 2900 configurations and 152 channels; the dimension of the Hamiltonian matrix was nearly 3000. Table 3 presents the entire list of the $(N+1)$-electron correlation configurations included (these need to be known

Table 1. Target terms and correlation configurations for Fe II. The values of the scaling parameters λ_{nl} for each orbital in the Thomas-Fermi-Dirac potential used in Superstructure are also given

Principal	Configurations:
$3s^2\ 3p^6\ 3d^6\ 4s$:	a ^{6}D, a ^{4}D, b ^{4}P, a ^{4}H, b ^{4}F, a ^{4}G, b ^{2}P, b ^{2}H, a ^{2}F, b ^{2}G, b ^{4}D, a ^{2}I, c ^{2}G, b ^{2}D, a ^{2}S, c ^{2}D
$3s^2\ 3p^6\ 3d^7$:	a ^{4}F, a ^{4}P, a ^{2}G, a ^{2}P, a ^{2}H, a ^{2}D, b ^{2}F
$3s^2\ 3p^6\ 3d^5\ 4s^2$:	a ^{6}S, b ^{4}G, d ^{4}P, c ^{4}D, ^{4}F
$3s^2\ 3p^6\ 3d^6\ 4p$:	z ^{6}D^0, z ^{6}F^0, z ^{6}P^0, z ^{4}F^0, z ^{4}D^0, z ^{4}P^0, z ^{4}S^0, y ^{4}P^0, z ^{4}G^0, z ^{4}H^0, z ^{2}D^0, z ^{4}I^0 y ^{4}D^0, z ^{2}G^0, y ^{4}F^0, z ^{2}I^0, x ^{4}D^0, y ^{4}G^0 z ^{2}F^0, y ^{2}G^0, z ^{2}P^0, z ^{2}H^0
$3s^2\ 3p^6\ 3d^5\ 4s\ 4p$:	z ^{8}P^0, y ^{6}P^0

Correlation configurations: $3p^6\ 3d^8\ 4s, 3s^2\ 3p^4\ 3d^9$, $3p^6\ 3d^7\ 4s\ 4p, 3s^2\ 3p^6\ 3d^6 4d, 3s^1\ 3p^6\ 3d^7\ 4p, 3s^1\ 3p^6\ 3d^8$, $3p^6\ 3d^9, 3s^2\ 3p^5\ 3d^7\ 4s, 3p^6\ 3d^7\ 4s^2, 3s^1\ 3p^6\ 3d^7\ 4s, 3s^2\ 3p^5\ 3d^8$
λ_{nl}: 1.33166 (1s), 1.23525 (2s), 1.07709 (2p), 1.07885 (3s), 1.05515 (3p), 1.05113 (3d), 1.03293 (4s), 0.88831 (4p), 1.40563 (4d).

Table 2. Calculated (cal) energy levels of Fe II and comparison with observed (obs) levels from Sugar & Corliss (1985). The energies (in Rydberg) are relative to the (^{5}D)4s a^{6}D ground state

	Level		$E_{\rm cal}$	$E_{\rm obs}$
1	(^{5}D) 4s	a ^{6}D	0.0	0.0
2	3d^7	a ^{4}F	0.0186	0.0182
3	(^{5}D) 4s	a ^{4}D	0.0953	0.0720
4	3d^7	a ^{4}P	0.1302	0.1203
5	3d^7	a ^{2}G	0.1604	0.1427
6	3d^7	a ^{2}P	0.1737	0.1651
7	3d^7	a ^{2}H	0.2146	0.1835
8	3d^7	a ^{2}D	0.1934	0.1861
9	(^{3}P)4s	b ^{4}P	0.2303	0.1914
10	(^{3}H)4s	a ^{4}H	0.2242	0.1918
11	(^{3}F)4s	b ^{4}F	0.2452	0.2040
12	3d^5 4s^2	a ^{6}S	0.2461	0.2087
13	(^{3}G)4s	a ^{4}G	0.2761	0.2310
14	(^{3}P)4s	b ^{2}P	0.2861	0.2347
15	(^{3}H)4s	b ^{2}H	0.2808	0.2354
16	(^{3}F)4s	a ^{2}F	0.2663	0.2463
17	(^{3}G)4s	b ^{2}G	0.3330	0.2746
18	(^{3}D)4s	b ^{4}D	0.3480	0.2825
19	3d^7	b ^{2}F	0.3279	0.2871
20	(^{1}I)4s	a ^{2}I	0.3475	0.2959
21	(^{1}G)4s	c ^{2}G	0.3608	0.3013
22	(^{3}D)4s	b ^{2}D	0.4059	0.3261
23	(^{1}S)4s	a ^{2}S	0.4145	0.3354
24	(^{1}D)4s	c ^{2}D	0.4115	0.3442
25	(^{5}D)4p	z ^{6}D^0	0.3515	0.3490
26	(^{5}D)4p	z ^{6}F^0	0.3732	0.3805
27	(^{5}D)4p	z ^{6}P^0	0.3798	0.3886
28	(^{5}D)4p	z ^{4}F^0	0.3872	0.4037
29	(^{5}D)4p	z ^{4}D^0	0.3807	0.4039
30	(^{5}D)4p	z ^{4}P^0	0.4012	0.4265
31	(^{6}S)4s4p	z ^{8}P^0	0.5667	0.4762
32	3d^5 4s^2	b ^{4}G	0.5462	0.4907
33	3d^5 4s^2	d ^{4}P	0.5961	0.5199
34	(^{3}P)4p	z ^{4}S^0	0.5762	0.5399
35	3d^5 4s^2	c ^{4}D	0.6237	0.5463
36	(^{3}P)4p	y ^{4}P^0	0.5805	0.5504
37	(^{3}H)4p	z ^{4}G^0	0.5729	0.5504
38	(^{3}H)4p	z ^{4}H^0	0.5760	0.5516
39	(^{3}P)4p	z ^{2}D^0	0.5850	0.5567
40	(^{3}H)4p	z ^{4}I^0	0.5756	0.5565
41	(^{3}P)4p	y ^{4}D^0	0.5849	0.5646
42	(^{3}H)4p	z ^{2}G^0	0.5801	0.5629
43	(^{3}F)4p	y ^{4}F^0	0.5955	0.5625
44	(^{6}S)4s4p	y ^{6}P^0	0.6379	0.5620
45	(^{3}H)4p	z ^{2}I^0	0.5816	0.5654
46	(^{3}F)4p	x ^{4}D^0	0.6002	0.5722
47	(^{3}F)4p	y ^{4}G^0	0.6020	0.5791
48	(^{3}F)4p	z ^{2}F^0	0.6025	0.5826
49	(^{3}F)4p	y ^{2}G^0	0.6096	0.5881
50	(^{3}P)4p	z ^{2}P^0	0.6015	0.5869
51	(^{3}H)4p	z ^{2}H^0	0.5983	0.5926
52	3d^5 4s^2	^{4}F	0.7699	0.6656

Table 3. Correlation functions for Fe I included in the CC expansion. Upper panel: correlations for quintets and singlets; lower panel: correlations for singlets and triplets

$3s^23p^63d^8$, $3s^23p^63d^74s$, $3s^23p^63d^74p$, $3s^23p^63d^74d$, $3s^23p^63d^64s4p$, $3s^23p^53d^84s$, $3p^63d^74s^24p$, $3s^23p^43d^94s$, $3p^63d^84s^2$, $3p^63d^94s$, $3s3p^63d^9$, $3s3p^63d^84s$, $3s^23p^63d^64p4d$, $3p^63d^94p$, $3s^23p^63d^64p^2$, $3s^23p^43d^74s4p^2$, $3s3p^53d^74s^24p$, $3s3p^63d^74s^2$, $3s^23p^53d^84p$, $3s^23p^63d^54s4p^2$, $3s3p^63d^64s4p^2$, $3s^23p^53d^64s4p^2$, $3s^23p^43d^64s^24p^2$, $3p^63d^64s^24p^2$, $3s^23p^43d^{10}$, $3p^63d^{10}$, $3s^23p^53d^74p^2$, $3s^23p^63d^64s^2$, $3s3p^63d^74p^2$, $3p^63d^84p^2$, $3p^63d^74s4p^2$, $3s^23p^63d^64s4d$, $3s^23p^43d^94d$, $3s^23p^43d^84s^2$, $3s^23p^43d^84s4p$, $3s3p^63d^84s$, $3p^63d^94s$, $3s^23p^53d^74s^2$, $3s3p^53d^84s^2$, $3s3p^53d^84s4p$, $3s3p^53d^84p^2$, $3s^23p^43d^74s^24p$, $3s^23p^53d^64s^24p$, $3s3p^63d^64s^24p$, $3s^23p^53d^54s^24p^2$, $3s3p^63d^54s^24p^2$, $3s3p^43d^74s^24p^2$, $3p^63d^84s^2$, $3s^23p^63d^54s^24p$, $3p^53d^84s^24p$, $3p^43d^84s^24p^2$, $3s^23p^43d^84s4p$, $3s3p^63d^84p$, $3s3p^53d^74s^24p$, $3p^63d^84p4d$, $3s^23p^43d^84p4d$ $3s^23p^43d^84p^2$
$3s^23p^63d^8$, $3s^23p^63d^74s$, $3s^23p^63d^74p$, $3s^23p^63d^74d$, $3s^23p^43d^74s^24p$, $3s3p^43d^94p^2$, $3s3p^43d^94s^2$, $3s^23p^63d^64s^2$, $3s^23p^63d^64s4p$, $3s^23p^53d^84s$, $3p^63d^74s^24p$, $3s^23p^43d^94s$, $3p^63d^84s^2$, $3s3p^63d^9$, $3s3p^63d^84s$, $3s^23p^53d^64s^24p$, $3p^63d^94p$, $3s^23p^63d^64p^2$, $3s^23p^43d^74s4p^2$, $3s3p^53d^74s^24p$, $3s3p^63d^74s^2$, $3s^23p^53d^84p$, $3s^23p^63d^54s4p^2$, $3s3p^63d^64s4p^2$, $3s^23p^53d^64s4p^2$, $3s^23p^43d^64s^24p^2$, $3p^63d^64s^24p^2$, $3s^23p^43d^{10}$, $3p^63d^{10}$, $3s^23p^53d^74p^2$, $3s3p^63d^74p^2$, $3s^23p^43d^84p^2$, $3p^63d^84p^2$, $3s3p^63d^64s^24p$, $3s^23p^63d^64s4d$, $3s^23p^43d^94d$, $3s^23p^43d^84s^2$, $3s^23p^43d^84s4d$, $3s^23p^53d^54s^24p^2$, $3p^63d^94s$, $3s^23p^53d^74s^2$, $3s3p^53d^84s^2$, $3s3p^53d^84s4p$, $3s3p^53d^84p^2$, $3s3p^43d^74s^24p^2$, $3s^23p^53d^74s4p$, $3p^43d^84s^24p^2$, $3s^23p^43d^84s4p$, $3s3p^63d^84p$, $3s3p^63d^54s^24p^2$, $3p^63d^84p4d$, $3s^23p^43d^84p4d$, $3s^23p^63d^64p4d$, $3s3p^63d^54s^24p$, $3p^53d^{10}4p$, $3p^53d^94s4p$, $3p^53d^84s^24p$, $3s^23p^53d^84p$, $3s^23p^53d^9$, $3s3p^53d^{10}$, $3s3p^53d^94p$, $3s3p^43d^{10}4s$, $3p^53d^{10}4p$, $3p^53d^94s4p$, $3p^63d^74s4p^2$

in order to reproduce or improve the present calculations and results).

4. Results

The results of the present calculations include the following sets of data: (a) energies of computed LS bound states of Fe I, (b) dipole oscillator strengths among all LS multiplets, and (c) total photoionization cross sections of the LS bound states, and partial cross sections for photoionization into specific states of Fe II (the ground state and several other excited states).

4.1. Energy levels

As the first step energies for bound state terms of Fe I are obtained, and a total of 1 117 states in LS coupling were found up to $n \leq 10$. Table 4 compares a small sample of

the computed energy levels separately for septets, quintets, triplets, and singlets with experimental values from Nave et al. (1994). The agreement for septets is good even for highly excited multiplets. the overall error of calculated energies with respect to observed values, weighted over the energy of the multiplet ($\sigma^2 = \sum \epsilon_{\rm obs}(\epsilon_{\rm obs} - \epsilon_{\rm cal})^2/\epsilon^2_{\rm obs}$), is about 1.9%. The agreement for quintet states can be regarded as satisfactory, particularly for terms with absolute energies greater than 0.2 Ry. It is noticed that the calculated energy for the a ^{5}D ground state of Fe I agrees with the observed energy to about 1.2%, and the averaged difference between calculated and observed energies weighted over the multiplet energies is about 4.4%. As expected, the results for the calculated energies of the triplets and singlets present the largest discrepancy with experiment. The overall difference with observed energies for triplets is about 8.9%. Calculated energies for singlet are in reasonable agreement with experiment for terms with absolute energy greater than 0.2 Ry; however, greater discrepancies are observed for higher excitation terms and the averaged difference with experiment is about 10.6%.

4.2. Oscillator strengths

Dipole oscillator strengths (f-values) for 32 316 transitions among the calculated states of Fe I were obtained in LS coupling. This set includes transitions when the lower state lies below the first ionization threshold and the upper state lies above. These transitions are important because they might contribute to the total photo-absorption, but do not appear as resonances in the photoionization cross sections.

There are two criteria commonly used in assessment of the accuracy of oscillator strengths. First, both length and velocity forms of the oscillator strengths are calculated and compared with each other. This provides a check on the accuracy of the wavefunctions and, therefore, on the accuracy of the f-values (Berrington et al. 1987). Figure 1 shows the log of the absolute value of the velocity form of the gf-values, plotted against the log of the length form of the gf-values separately for septets, quintets, triplets, and singlets. In each panel the statistical dispersion of the plot for $gf_{\rm L} \geq 0.01$ is indicated. It is observed that dispersion in the gf-values for each symmetry is consistent with the differences found between the calculated energies and the experimental ones. Septets, whose calculated energies agree well with experiment, exhibit the lowest dispersion in the gf-values of only 11%. Transitions among quintet terms have a greater dispersion of about 20%. Triplets present the largest dispersion ($\sim 51\%$) consistently with the discrepancies found for the energy levels; however, for transitions with $gf_{\rm l} \geq 0.1$ the dispersion is about 22%. The dispersion for transitions among singlet states is about 27%. The second accuracy evaluation is the comparison of a limited number of individual gf values with those observed experimentally by Nave et al. (1994), and those in the critical compilation of transition probabilities by Fuhr et al. (1988). For this comparison, presented in Table 4, the fine structure gf values presented by Nave et al. and Fuhr et al. were summed, though for some multiplets the experimental data is incomplete. Some improvement to the accuracy of the calculated gf values can be obtained by correcting the calculated energy difference for the transitions with experimental energies, i.e.

$$gf_{ij}({\rm cor}) = \frac{(E_j - E_i)_{\rm exp}}{(E_j - E_i)_{\rm cal}} \times gf_{ij}({\rm cal}), \qquad (3)$$

where gf_{ij}(cor) and gf_{ij}(cal) are the corrected and calculated gf-values respectively and $(E_j - E_i)_{\rm exp}$ and $(E_j - E_i)_{\rm cal}$ are the experimental and calculated energy differences between the levels.

Table 5 shows some significant differences with the two sources of experimental data. In most cases these differences arise from incompleteness of the set of fine structure f-values, measured within an LS multiplet, in the earlier compilation by Fuhr et al. (1988) as compared to the more complete work by Nave et al. (1994). In some other cases, however, differences up to 40% come from the experimental measurements themselves. It is also noted that the effect of correcting the calculated gf-values using experimental energy differences is quite significant, and in most cases seems to bring the gf-values closer to those measured experimentally. Unfortunately, it is difficult to derive conclusions regarding the accuracy of the gf-values for transitions among septets since there seems to be no complete experimental data for any multiplets. Thus the values given in Table 5, summed over the available fine structure components, should be considered as lower limits to the total LS multiplet strength. Oscillator strengths for quintets compare reasonably well with experiment, the differences being within $10-20\%$ with only two exceptions. Once again, triplets and singlets present the largest discrepancies with respect to observed values, though most values are in good agreement, $10-20\%$, with experiment.

The dispersion between length and velocity forms of the oscillator strengths and the comparison of a sample of values with experimental measurements suggests that for septets and quintets the present gf may be accurate to the $10-20\%$, gf-values for singlets to about 30%, and for triplets to about $30-50\%$. The present gf-values could be considerably improved if corrected using experimental energy separations; this is recommended for practical applications.

4.3. Photoionization cross sections

The importance of including ionization of the inner 3d shell in the calculation of photoionization cross sections of Fe I was investigated in a previous paper (Bautista & Pradhan 1995). Figures 1a and 1b of this paper show that when the inner-shell ionization channels into $3d^54s^2$ and $3d^54s4p$ terms of Fe II are included in the CC expansion,

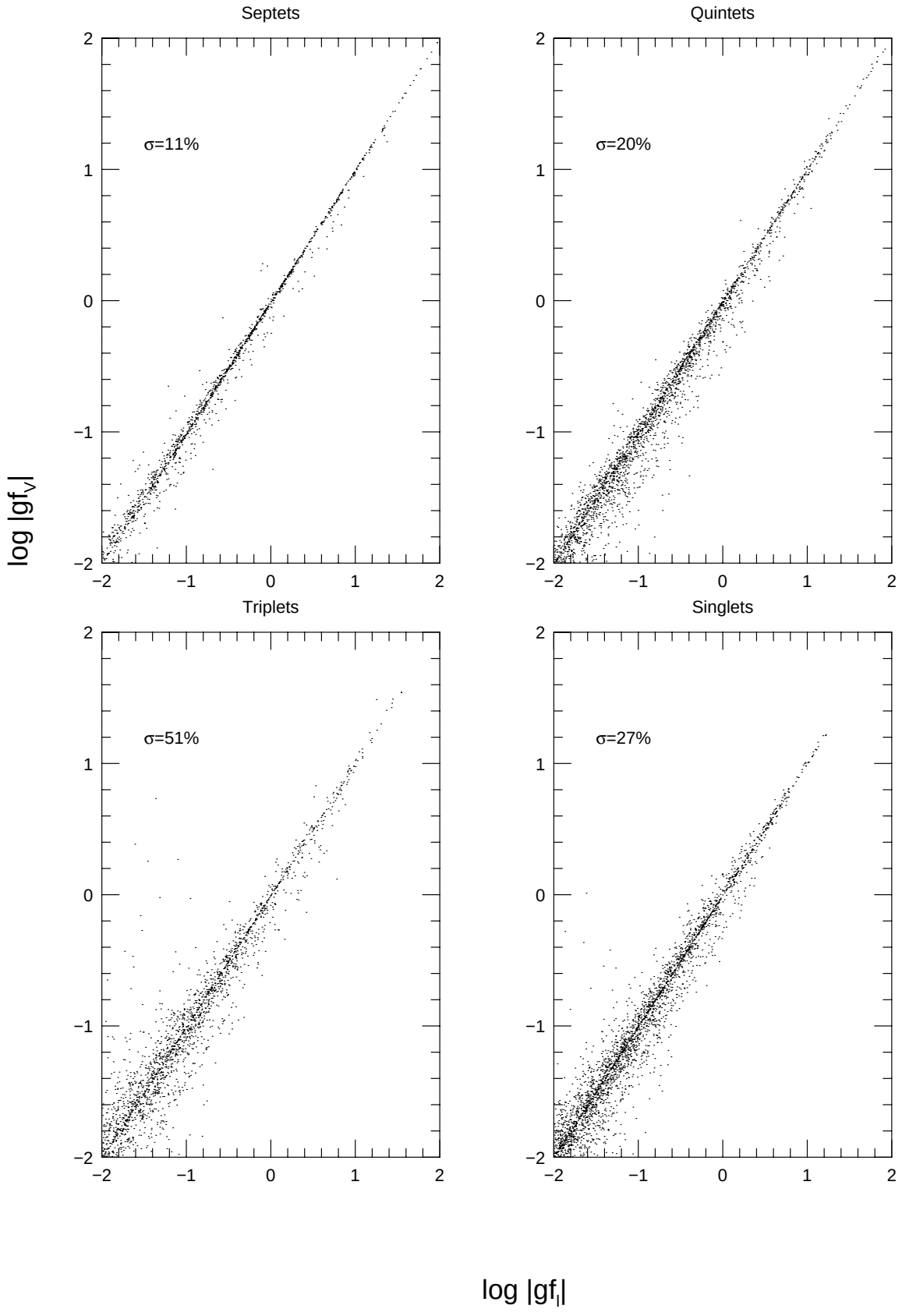

Fig. 1. log $gf_{\rm V}$ plotted against log $gf_{\rm L}$ for transitions between calculated LS terms

Table 4. Comparison of calculated (cal) energy levels in Ry with the observed (obs) levels from Nave et al. (1994)

Conf.	Term	$-E_{\rm cal}$	$-E_{\rm obs}$	Conf.	Term	$-E_{\rm cal}$	$-E_{\rm obs}$
$3d^6(^5D)4s4p$	z^7D^o	0.4130	0.4020	$3d^6(^5D)4s4p$	z^7F^o	0.3850	0.3719
$3d^6(^5D)4s4p$	z^7P^o	0.3750	0.3616	$3d^5(^6S)4s^24p$	y^7P^o	0.2130	0.2139
$3d^6(^5D)4s(^6D)5s$	e^7D	0.1850	0.1869	$3d^6(^5D)4s(^6D)5p$	$^7D^0$	0.1260	0.1283
$3d^6(^5D)4s(^6D)4d$	e^7P	0.1200	0.1196	$3d^6(^5D)4s(^6D)4d$	f^7D	0.1210	0.1185
$3d^6(^5D)4s(^6D)4d$	e^7S	0.1180	0.1109	$3d^6(^5D)4s(^6D)6s$	g^7D	0.0880	0.0869
$3d^64s^2$	a^5D	0.5700	0.5771	$3d^7(^4F)4s$	a^5F	0.5290	0.5128
$3d^7(^4P)4s$	a^5P	0.4280	0.4197	$3d^6(^5D)4s4p$	z^5D^o	0.3620	0.3425
$3d^6(^5D)4s4p$	z^5F^o	0.3470	0.3328	$3d^6(^5D)4s4p$	z^5P^o	0.3320	0.3135
$3d^7(^4F)4p$	y^5D^o	0.2810	0.2755	$3d^7(^4F)4p$	y^5F^o	0.2770	0.2699
$3d^7(^4F)4p$	z^5G^o	0.2660	0.2606	$3d^6(^5D)4s4p$	y^5P^o	0.2420	0.2434
$3d^6(^5D)4s4p$	x^5D^o	0.2190	0.2166	$3d^6(^5D)4s4p$	x^5F^o	0.2190	0.2104
$3d^6(^3P)4s4p$	z^5S^o	0.2000	0.2081	$3d^6(^3P)4s4p$	x^5P^o	0.1770	0.1912
$3d^6(^3P)4s4p$	w^5D^o	0.1730	0.1807	$3d^6(^3F)4s4p$	$^5D^o$	0.1540	0.1770
$3d^6(^5D)4s(^6D)5s$	e^5D	0.1660	0.1703	$3d^6(^3F)4s4p$	x^5G^o	0.1390	0.1637
$3d^7(^4F)5s$	e^5F	0.1460	0.1479	$3d^6(^3G)4s4p$	w^5G^o	0.0810	0.1477
$3d^6(^5D)4s(^6D)4d$	f^5D	0.1260	0.1198	$3d^6(^5D)4s(^6D)4d$	e^5G	0.1250	0.1173
$3d^6(^5D)4s(^6D)5p$	u^5F^o	0.1120	0.1122	$3d^6(^5D)4s(^6D)4d$	f^5F	0.1160	0.1121
$3d^6(^5D)4s(^6D)4d$	e^5P	0.1110	0.1074	$3d^7(^4F)5p$	$^5F^o$	0.0960	0.0959
$3d^7(^4F)4d$	h^5D*	0.0770	0.0927	$3d^7(^4F)4d$	g^5F	0.0780	0.0925
$3d^7(^4F)4s$	a^3F	0.4730	0.4677	$3d^64s^2$	a^3P	0.3880	0.4081
$3d^64s^2$	a^3H	0.3490	0.4024	$3d^64s^2$	b^3F	0.3490	0.3911
$3d^7(^2G)4s$	a^3G	0.3690	0.3808	$3d^7(^4P)4s$	b^3P	0.3600	0.3721
$3d^64s^2$	b^3G	0.2970	0.3617	$3d^7(^2P)4s$	c^3P	0.3460	0.3570
$3d^7(^2H)4s$	b^3H	0.3160	0.3409	$3d^7(^2D2)4s$	a^3D	0.3290	0.3403
$3d^64s^2$	b^3D	0.2440	0.3133	$3d^6(^5D)4s4p$	z^3D^o	0.3070	0.2932
$3d^6(^5D)4s4p$	z^3F^o	0.2970	0.2922	$3d^8$	c^3F	0.2080	0.2777
$3d^6(^5D)4s4p$	z^3P^o	0.2810	0.2696	$3d^7(^4F)4p$	z^3G^o	0.2590	0.2556
$3d^7(^2F)4s$	d^3F^o	0.0940	0.2437	$3d^7(^4F)4p$	y^3F^o	0.2430	0.2432
$3d^7(^4F)4p$	y^3D^o	0.2270	0.2299	$3d^8$	^3P	0.0380	0.2071
$3d^6(^3P)4s4p$	z^3S^o	0.1260	0.1562	$3d^6(^3P)4s4p$	y^3P^o	0.1400	0.1545
$3d^6(^3F)4s4p$	$^3F^o$	0.0570	0.1522	$3d^7(^4P)4p$	y^3S^o	0.1190	0.1475
$3d^7(^4P)4p$	x^3P^o	0.1180	0.1398	$3d^7(^2G)4p$	w^3F^o	0.1250	0.1322
$3d^6(^3F)4s4p$	$^3F^o$	0.0570	0.1522	$3d^7(^4P)4p$	y^3S^o	0.1190	0.1475
$3d^7(^4P)4p$	x^3P^o	0.1180	0.1398	$3d^7(^2G)4p$	w^3F^o	0.1250	0.1322
$3d^7(^2G)4p$	v^3G^o	0.0970	0.1287	$3d^7(^2P)4p$	w^3P^o	0.0910	0.1241
$3d^7(^2G)4s$	a^1G	0.3470	0.3569	$3d^7(^2P)4s$	a^1P	0.3330	0.3298
$3d^7(^2D2)4s$	a^1D	0.3170	0.3201	$3d^7(^2H)4s$	a^1H	0.2930	0.3182
$3d^64s^2$	a^1I	0.2830	0.3137	$3d^64s^2$	b^1G	0.3000	0.3093
$3d^64s^2$	b^1D	0.2540	0.2652	$3d^6(^3P)4s4p$	$^1D^o$	0.1370	0.1487
$3d^6(^3H)4s4p$	y^1G^o	0.1100	0.1370	$3d^6(^3F)4s4p$	$^1F^o$	0.1080	0.1322
$3d^6(^3H)4s4p$	$^1H^o$	0.0800	0.1103	$3d^7(^2P)4p$	y^1D^o	0.0730	0.1096
$3d^7(^2H)4p$	z^1I^o	0.1130	0.0970	$3d^6(^3G)4s4p$	y^1H^o	0.0430	0.0913

both the background and the resonance structures of the photoionization cross sections of Fe I are considerably enhanced. Moreover, the CC result including coupling to the 3d subshell differs by more than three orders of magnitude in the energy region below about 1 Ry from earlier results by Reilman & Manson (1979) using the central field approximation and Verner et al. (1993) in the Dirac-Hartree-Slater approximation. This is because both of these approximations neglect the complex correlation effects, such as the coupling to inner-shell channels, that give rise to an unphysical discontinuous jump of several orders of magnitude. For energies of the ionizing photon greater than 1 Ry our results agree well with these earlier results.

Figure 2 compares the present ground state cross section with that from Kelly & Ron (1972) and Kelly (1972). The first of these papers concerns the small range of energy from the ionization threshold to 10 eV ($\sim$ 0.735 Ry), and the second paper deals with the cross section for a more extended range of energies. The agreement between the present work and both of these cross sections is remarkably good below 0.73 Ry, where the cross section is dominated by correlations involving the terms of the core ion $3d^6(^5D)4s$ a ^6D, $3d^7$ a ^4F, $3d^6(^5D)4s$ a ^4D, and $3d^7$ a ^4P. Beyond this energy Kelly's calculations underestimate the actual cross section; most likely due to missing correlations from the $3d^6(^3P)4s\,^4P$, $3d^6(^3H)4s\,^4H$, $3d^6(^3F)4s\,^4F$, $3d^6(^3G)4s\,^4G$ and $3d^6(^3D)4s\,^4D$ terms. Nevertheless, Kelly included contributions from $3d^54s^2(^6S)$ that produce a sharp jump of the cross section near 0.79 Ry. An interesting feature in

Table 5. Comparison of calculated and corrected gf-values with experimental measurements from Nave et al. (1994) and Fuhr et al. (1988)

Transition	Present[1]	Present[2]	Nave et al.	Fuhr et al.
$z^7D^o - e^7D$	5.44	5.13	4.32	3.47 *
$f^7D - z^7F^o$	0.334	0.320		0.560*
$z^7D^o - e^7F$	12.4	12.1	7.14*	4.32*
$e^7F - z^7F^o$	2.18	2.11	3.08*	1.98*
$z^7D^o - f^7D$	7.40	10.2	5.06*	
$e^7F - e^7D$	8.26	7.63	6.41*	
$e^7F - e^7G$	18.3	17.7	11.7*	
$a^5D - z^5D^o$	0.689	0.611	0.575	0.566
$a^5D - z^5F^o$	1.26	1.20	1.12	0.371*
$a^5D - z^5P^o$	0.598	0.540	0.611	0.162*
$a^5D - y^5D^o$	3.67	3.52	3.29	2.28*
$a^5D - y^5F^o$	1.56	1.49	1.46	1.41*
$a^5D - y^5P^o$	5.16	5.07	2.81*	3.06*
$a^5D - x^5P^o$	0.0739	0.0753	0.110	0.190*
$a^5D - x^5F^o$	15.9	15.2	15.5	14.2*
$a^5D - x^5D^o$	8.26	8.04	7.05	7.63*
$a^5F - z^5D^o$	0.243	0.238	0.174	0.166*
$a^5F - z^5F^o$	0.0223	0.0221	0.0121	0.0115*
$a^5F - z^5G^o$	10.6	10.2	6.64*	6.30 *
$a^5F - y^5D^o$	4.70	3.86	3.62	3.60 *
$a^5F - y^5F^o$	8.14	7.85	6.75	6.75
$a^5P - z^5P^o$	0.233	0.258	0.196	0.137*
$a^5P - z^5S^o$	0.686	0.636	0.325	0.316
$a^5P - y^5D^o$	0.0183	0.0179	0.031	0.0263
$a^5P - y^5P^o$	0.0791	0.0746	0.0506	0.0425*
$a^5P - x^5P^o$	0.282	0.256	0.213	0.245
$a^3F - z^3F^o$	0.0385	0.0383	0.0444	0.0400*
$a^3D - y^3F^o$	6.17	6.98	5.15	5.25
$a^3F - z^3D^o$	0.270	0.283	0.206	0.100*
$a^3F - y^3D^o$	5.24	5.11	4.44	4.68*
$a^3P - z^3P^o$	0.0664	0.0494	0.0252	0.025
$a^3F - y^3G^o$	0.243	0.206	0.183*	
$a^3G - z^3F^o$	0.618	0.364	0.211*	
$a^3G - x^3G^o$	0.282	0.261	0.173	
$a^3G - v^3G^o$	3.81	3.53	3.42	
$a^1G - z^1G^o$	0.618	0.578	0.186	0.158
$a^1G - y^1G^o$	0.616	0.587	0.631	
$a^1G - z^1H^o$	2.19	1.58	1.44	1.78
$a^1G - z^1F^o$	0.224	0.210	0.575	0.724
$a^1G - y^1G^o$	0.616	0.572	0.631	
$a^1G - x^1G^o$	0.802	0.747	0.468	0.562
$a^1G - x^1F^o$	0.639	0.512	0.316	0.347
$a^1P - w^1D^o$	0.324	0.274	0.170	0.170
$a^1D - z^1F^o$	0.158	0.136	0.0978	0.166
$a^1D - y^1D^o$	0.159	0.137	0.158	0.11
$a^1D -^1 P^o$	0.0616	0.0646	0.0537	0.0457
$a^1G - w^1G^o$	0.793	0.713	0.851	

[1] calc. with theoretical energies
[2] corrected with obs. energies
* incomplete multiplet.

Kelly's cross section is the series of resonances due to $3d^54s^2np\ ^5P,^5D,^5F$ autoionizing states (see Fig. 7 of Kelly & Ron 1972). The position of the strongest set of these resonances obtained by Kelly was about 0.89 Ry while the actual structure of the peak and its hight were rather uncertain. The present calculations reproduce such a feature but at 0.94 Ry and it is considerably higher than in Kelly's results. Some other resonances of this series found by Kelly are also seen in the present cross section. Another important characteristic of the cross section is its sharp jump at the position of the thresholds for ionization of the inner 3d subshell. Kelly's calculations give a single edge at 1.16 Ry for all the contributions due to $3d^54s^2\ ^4P,^4D,^4F$, and ^4G. In the present calculation separate edges are obtained for each of these thresholds, as well as for those of $3d^6(^6D)4s4p\ ^8P^o$, and $^6P^o$ which were not

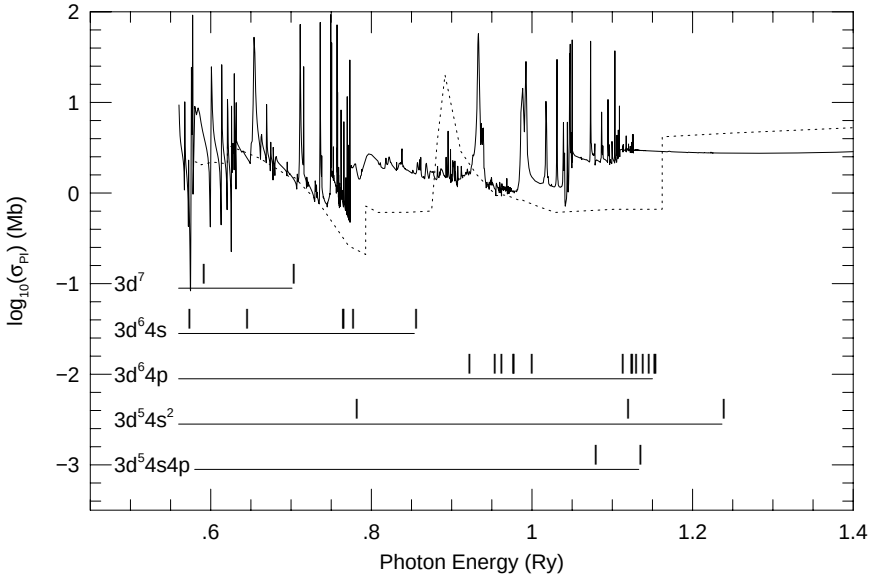

Fig. 2. Photoionization cross section (σ (Mb)) of the ground state $3d^6 4s^2\ ^5D$ of Fe I as a function of photon energy in Ry: full curve, present result; broken curve, Kelly (1972). Thresholds from all electronic configurations included in present computation are marked

considered by Kelly. Finally, Kelly's cross section at high energies (above the thresholds associated with 3d inner-shell ionization) agrees well with both the present results and those from central field type approximations (Reilman & Manson 1979; Verner et al. 1993).

Photoionization cross sections were calculated for all computed bound states with energy below the first ionization potential of Fe I. In order to delineate in detail the autoionization resonances near the ionization thresholds a very fine mesh of energies, typically about 2000 points, was used in the range of up to 0.3 Rydberg above the threshold. Figure 3 shows the photoionization cross section of the two lowest excited terms of Fe I $3d^7(^4F)4s\ a^5F$, and $3d^7(^4F)4s\ a^3F$.

In practical applications, particularly non-LTE spectral models, it is important to determine accurately the level population in the *excited* levels of the residual ion following photoionization. Therefore, partial cross sections for photoionization of the ground state of Fe I into the ground and excited terms of Fe II have been calculated. A few examples of these partial cross sections were given in an earlier paper (Bautista & Pradhan 1995). Also in that paper, we show examples of the so called photoexcitation-of-core (PEC) resonances in photoionization cross sections along Rydberg series of Fe I. Such PEC resonances result from strong dipole couplings between opposite parity terms within the target ion (Yu & Seaton 1987). The present work entails the full set of calculations for all 1 117 bound states, including partial cross sections into the ground and excited states with multiplicity $(2L+1) = 5$ and 7 of Fe II.

5. Conclusion

Extensive radiative data: energy levels, dipole oscillator strengths, and partial and total photoionization cross sections for Fe I are presented. Most of these data were calculated for the first time and are expected to provide a reasonably complete dataset for Fe I to be used in astrophysical models.

Total and partial photoionization cross sections for all bound states of Fe I have been obtained, carefully delineating the autoionizing resonance structures. The cross section of the ground state, $4s^2\ ^5D$, was compared with previous theoretical calculations in central field approximations and differences of over *three orders of magnitude* were found. Much better agreement for this cross section was found with earlier work by Kelly & Ron (1972) and Kelly (1972) using the many-body perturbation theory.

All the data reported here should be available in the near future from the Opacity Project data server TOPbase (Cunto et al. 1995; Mendoza 1995, private communication).

The complexity of the present computations can be inferred from the fact that they required two years of almost uninterrupted computations and about 1500 CPU hours on the Cray Y-MP8/64.

Acknowledgements. I would like to thank Prof. Anil Pradhan for suggesting this work and for discussions and comments. I also appreciate the assistance of Dr. Sultana Nahar for the identification of bound states. This work was supported in part by the U.S. National Science Foundation (PHY-9421898) grant for the IRON Project. The computations were carried out on the Cray YMP8 at the Ohio Supercomputer Center (OSC).

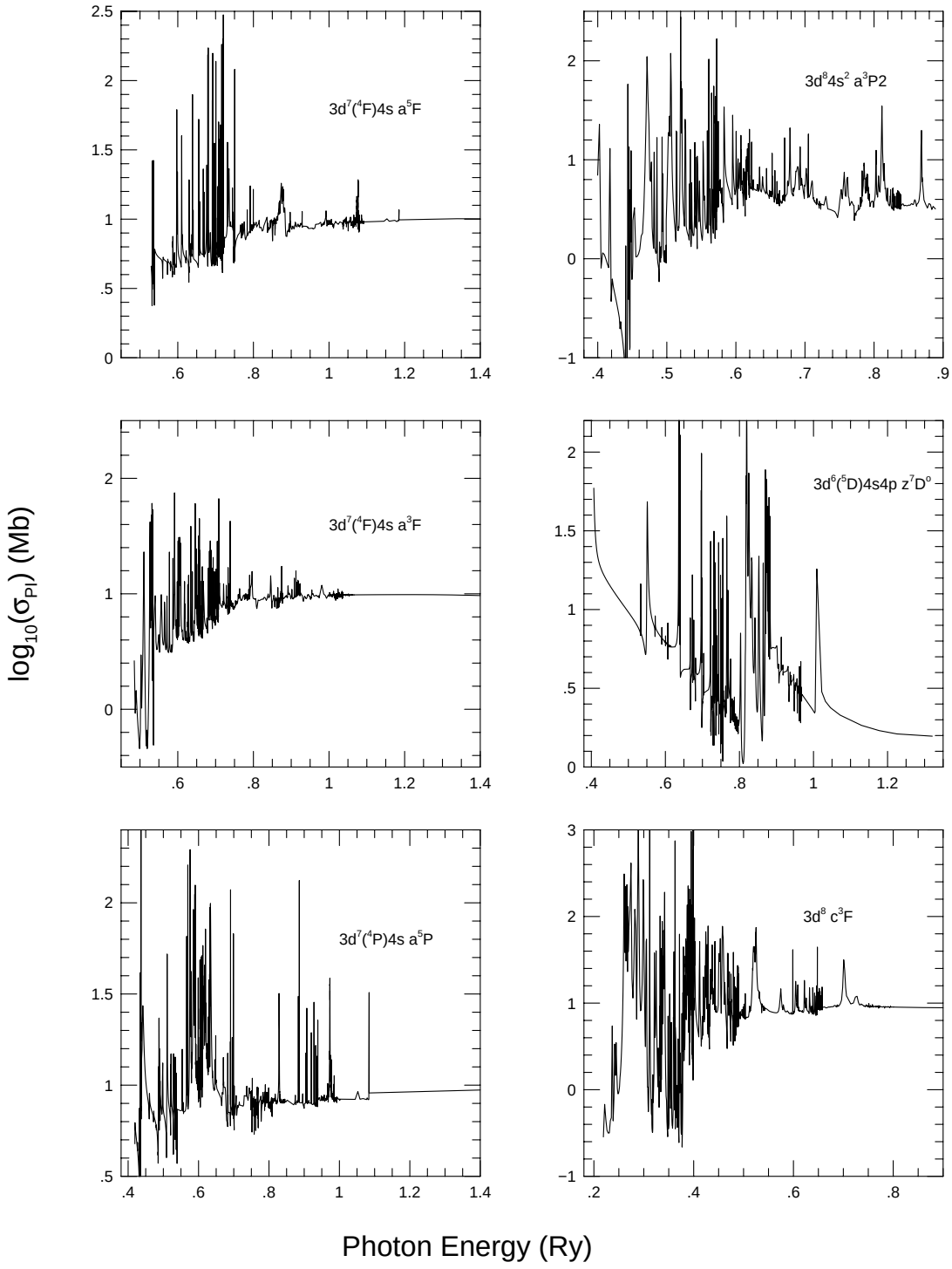

Fig. 3. Photoionization cross sections (σ (Mb)) as a function of photon energy in Ry for a sample of excited states of Fe I

References

Bautista M.A., 1996, A&AS 119, 105

Bautista M.A., Pradhan A.K., 1995, J. Phys. B: At. Mol. Phys. 28, L173

Bautista M.A., Nahar S.N., Peng J.F., Pradhan A.K., Zhang H.L., 1995, in Astrophysics in the Extreme Ultraviolet, Bowyer S. (ed.) IAU Symposium, No. 152

Bell R.A., Paltoglou G., Tripicco M.J., 1994, MNRAS 268, 771

Berrington K.A., Burke P.G., Butler K., Seaton M.J., Storey P.J., Taylor K.T., Yu Yan, 1987, J. Phys. B: At. Mol. Phys. 20, 6379

Cunto W., Mendoza C., Ochsenbein F., Zeippen C.J., 1993, A&A 275, L5

Eissner W, Jones M., Nussbaumer H., 1974, Comput. Phys. Commun. 8, 270
Fuhr J.R., Martin G.A., Wiese W.L., 1988, J. Phys. Chem. Ref. Data 17, Suppl. 4
Hummer D.G., Berrington K.A., Eissner W., Pradhan A.K., Saraph H.E., Tully J.A., 1993, A&A 279, 298
Kelly H.P., 1972, Phys. Rev. A 6, 1048
Kelly H.P., Ron A., 1972, Phys. Rev. A 5, 168
LeBlanc F., Michaud G., 1995, A&A 303, 166
Nahar S.N., 1995a, A&A 293, 967
Nahar S.N., 1995b, A&AS (submitted)
Nahar S.N., Pradhan A.K., 1994, J. Phys. B: At. Mol. Phys. 27, 429
Nave G., Johansson S., Learner R.C.M., Thorne A.P., Brault J.W., 1994, ApJS 94, 221
Nussbaumer H., Storey P.J., 1978, A&A 64, 139
Pradhan A.K., 1995, in Astrophysics in the Extreme Ultraviolet, Bowyer S. (ed.), IAU Symposium, No. 152
Reilman R.F., Manson S.T., 1979, ApJS 40, 815
Sawey P.M.J., Berrington K.A., 1992, J. Phys. B: At. Mol. Phys. 25, 1451
Seaton M.J., Yu Yan, Mihalas D., Pradhan A.K., 1994, MNRAS 266, 805
Sugar J., Corliss C., 1985, J. Phys. Chem. Ref. Data 14, Suppl. 2
Verner D.A., Yakovlev D.G., Band I.M., Trzhaskovskaya M.B., 1993, At. Data. Nucl. Data Tab. 55, 233
Yu Yan, Seaton M.J., 1987, J. Phys. B: At. Mol. Phys. 20, 6409